J. Mater. Environ. Sci.6 (7) (2015) 1858-1864
ISSN : 1503-1755
CODEN: JMESCN

Characterization of bionanomaterial Ni_{60}-Cr_{40} alloy obtained by mechanical alloying

L. Dekhil [1, *], N. Zerniz[2], M. Bououdina[3], N. Haneche[4], E.B. Haneche[5], J. M. Grenèche[6]
[1] Laboratoire de Mise en forme des Matériaux Métalliques (LMF2M), Département de Métallurgie, Faculté des Sciences de l'ingéniorat, Université Badji Mokhtar, B.P.12,23000, Annaba, Algeria.
[2] Laboratoire de Chimie organique, Département de Chimie, Faculté des Sciences, Université Badji Mokhtar, B.P.12, 23000, Annaba, Algérie.
[3] Department of Physics, College of Science, University of Bahrain, PO Box 32038, Kingdom of Bahrain.
[4] Institut des Molécules et des Matériaux du Mans, Université du Maine, Faculté des Sciences 72085, Le Mans Cedex 9, France.
[5] Laboratoire LESIMS, Département de Physique, Faculté des Sciences, Université Badji Mokhtar, B P.12, 23000 Annaba, Algérie.
[6] Laboratoire de Physique de l'état condensé- UMR6087, Université du Maine, Faculté des Sciences 72085, Le Mans Cedex 9, France.

Received 25 Jan 2015, Revised 12 May 2015, Accepted 12 May 2015
[*] *Corresponding Author. E-mail: l.dekhil@gmx.com*

Abstract

Ni60-Cr40 powder mixtures were prepared from elemental Ni and Cr using a high energy ball mill (Fritsh P7) under an argon atmosphere. Microstructural, structural, magnetic and mechanical properties were followed by scanning electron microscopy, vibrating sample magnetometry and Vickers micro-hardness measurements. Morphological observations show the existence of a broad distribution of size and shape of the powder particles. After 6 h of milling, the Rietveld refinement of X-ray diffraction pattern reveals the formation of disordered Cr(Ni) solid solution. The crystallite size refinement against the milling time is accompanied by an increase of the atomic level strain. Cold compacting followed by liquid phase sintering were carried out in order to obtain a bulk sample and to estimate both porosity percentage and powders formability. Due to the coexistence of different microstructural components and their interactions, multiphase alloy offers an excellent combination between high formability and hardness.

Key words: Ni-Cr alloy; Bionanomaterial; XRD; SEM; VSM; Sintering; Micro-hardness.

1. Introduction

Significant progress has been made in order to understand fundamental aspects of the nanomaterials synthesis. Thus, various processing routes have been adopted for their production including vapor-solid-liquid approach [1], equal channel angular pressing (ECAP) [2] and high energy ball milling [3-5]. Among various biomaterials alloys, Ni–Cr alloys have excellent high temperature strength and good corrosion resistance. The excellent properties of Ni–Cr alloys are due to their complex composition. They are widely used in electrical elements and dental applications [3–5]. Generally, these alloys are composed of Ni (68–80%) and Cr (11.9–26.3%), but alloying with other elements is required to ensure the achievement of mechanical strength and corrosion resistance and porcelain bonding. Iron, aluminum, molybdenum, silicon, beryllium, magnesium, cobalt carbon, niobium, copper, titanium, gallium, magnesium and tin are added to Ni–Cr alloys in the range of 0.1–14 wt. % [6]. The casting of these alloys is easily performed by the use of a gas-oxygen flame with a blowtorch. However, the gas–air combustion in the blowtorch exposes noble, nickel–chromium and other alloys [7,8] to oxidation through the inclusion of carbon, which might change the physical properties of Ni–Cr alloys [9]. The aim of the present study is to produce nanostructured Ni_{60}-Cr_{40} powders by high energy ball milling process. To follow the evolution of structural, microstructural and magnetic properties of mechanically alloyed Ni-Cr powder mixtures by means of X-ray diffraction, thermal stability, magnetic measurement and micro-hardness.

2. Experimental details

High purity elemental Ni (3 µm, 99, 8 %) and Cr (< 8 µm) powders with a nominal composition of Ni_{60}-Cr_{40} (wt.%) were mechanically alloyed in a planetary ball mill (Fritsch Pulverisette 7) under argon atmosphere using hardened steel balls and vials. The ball-to- powder weight ratio was about 35/5 and the rotation speed was 400 rpm. To avoid the excessive temperature increase inside the vials, the milling process was interrupted each 1/2 h for 1/4 h.The morphological changes of the powder particles were followed by SEM in DSM960A Zeiss equipment. Structural evolution and phase transformation were investigated by X-ray diffraction (XRD) by means of Siemens D501 diffractometer in a *(θ-2θ)* Bragg Brentano geometry using Cu-Kα radiation (λ = 0.154056 nm). Morphological changes of the powder particles during the milling process were followed by scanning electron microscopy (SEM) in a DSM960 A Zeiss equipment. Magnetic properties were determined by measuring M-H hysteresis loops using a vibrating sample magnetometer VSM 3900 PMC under an applied field of 1 T at 300 K.

3. Results and discussion

3.1. SEM analysis

The progressive change in morphology during the milling process is due to the repeated fracturing, cold-welding, agglomeration and de-agglomeration of powder particles. Fig. 1 shows the SEM micrographs of the Ni_{60}-Cr_{40} powders after various milling times.

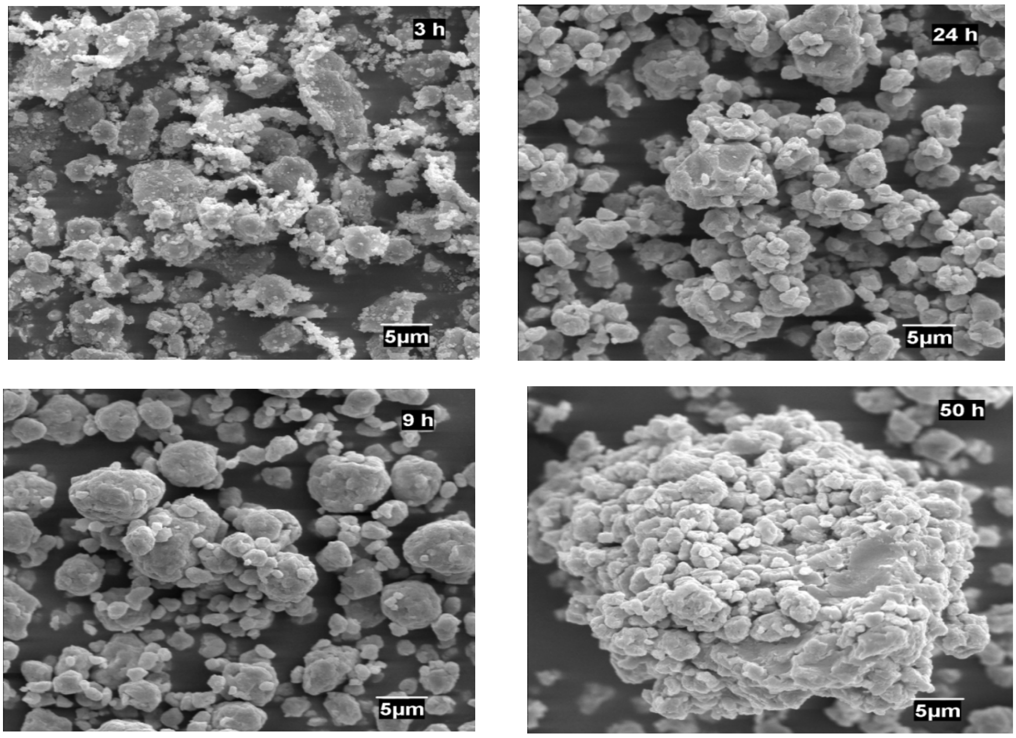

Fig. 1. Morphological changes of the Ni-Cr powder particles as a function of milling time.

At the early stage of milling, the ductile powders can easily be plastically deformed under compressive forces, and consequently, they become flattened into flakes through micro-forging (3 h). Also, since the powders are soft they tend to agglomerate by cold welding and form bigger particles with a diameter of about 10 µm (6 h). At the intermediate stage of milling, fracturing is the main event involved in the MA process. Therefore, the agglomerated powder particles are subject to continuous disintegration with fragmentation to form relatively fine powders with particles size smaller than 12 µm in diameter (24 h). Further milling time leads to roughly spherical agglomerate composite particles having nearly the same shape but varying in size from about 1.3 to 12.6 µm in diameter. The induced heavy plastic deformation into the powder particles, during the milling process, gives rise to the creation of a great amount of crystal defects such as dislocations, vacancies, interstitials and grain boundaries which promote solid state reaction at ambient temperature. Depending on the initial mixture, changes in structures of mechanically alloyed powders can occur as follows: grain refinement, solid solution diffusion and/or formation of new phases. The weak force area supports the fragmentation of the powder particles strongly hardened by the tiredness mechanism. So, the fracture dominates welding at this stage what leads to a narrow distribution. The competition between welding and fracture is evidenced by the coexistence of agglomerates and fine particles after 50 h of milling. The size distribution of the powder particles was estimated by statistics made on SEM micrographs at various times of crushing (figure2).

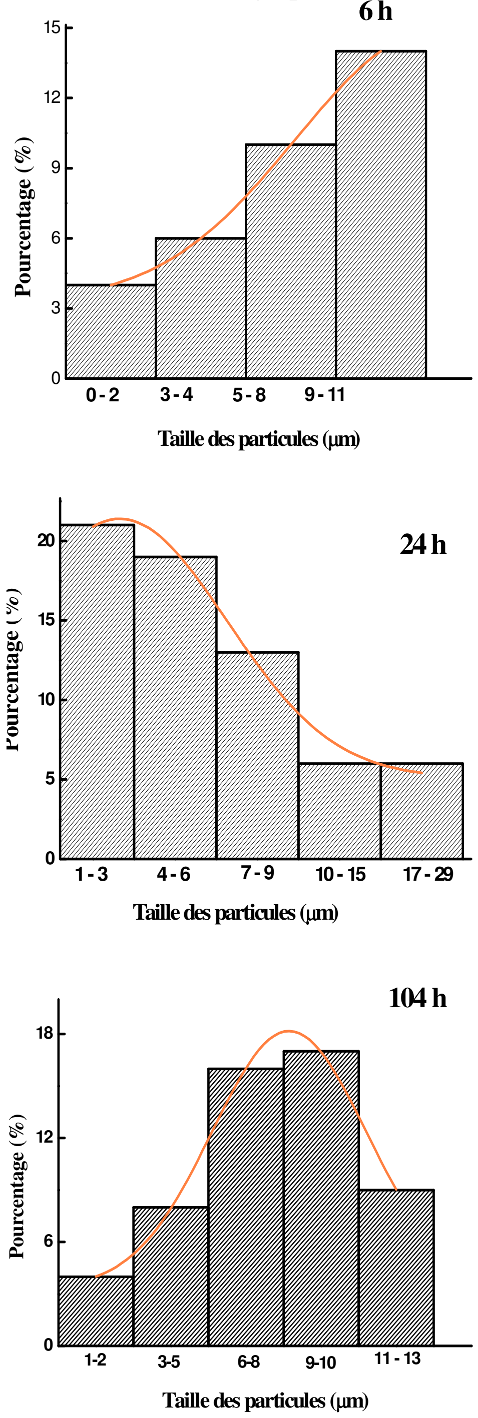

Fig. 2. Evolution of crystallite size distribution as a function of milling time

After 6 h, the distribution moves towards the big sizes with a maximum of approximately 13% in the interval (12-36) µm. The predominance of the phenomenon of fracture is confirmed by the displacement of the maximum of the distribution towards sizes about (5 – 7) µm and (1-3) µm after 9 and 24 h of milling, respectively. Prolonged milling (24 h) led to a narrow distribution of Gaussian form of which the maximum is centered on (8-9) µm approximately.

The evolution of the average size of the powder particles with the milling time (Fig. 3) presents three distinct stages which clearly reflect the competition between welding phenomena and refinement. Thus the fast increase until 6 h, the reduction between 6 and 24 h and the increase up to 104 h of milling can be explained by the predominance of cold welding, fractures and rewelding respectively.

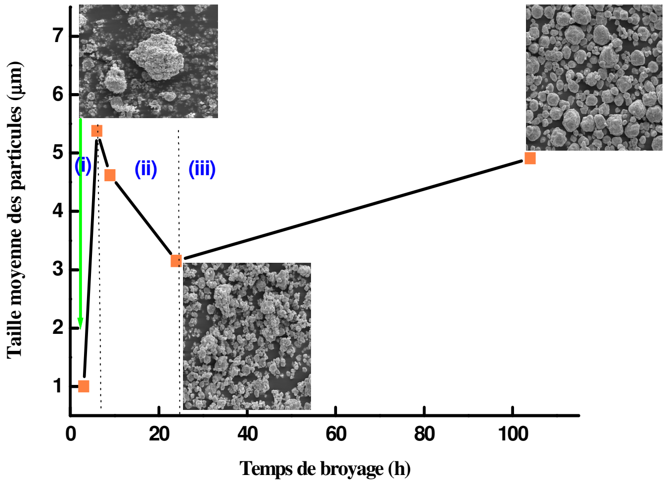

Fig. 3. Evolution of average crystallite size as a function of milling time

3.2. Magnetic properties

The hysteresis loops of the Ni-Cr powders milled for several times are characterized by a sigmoidal form (Fig. 4). The small hysteresis losses are properties desired in soft magnetic materials and usually observed in nanostructured samples. The coercivity, Hc, depends strongly on the particle size, morphology, chemical composition and the large fraction of atoms associated with the grain boundaries/interfaces.

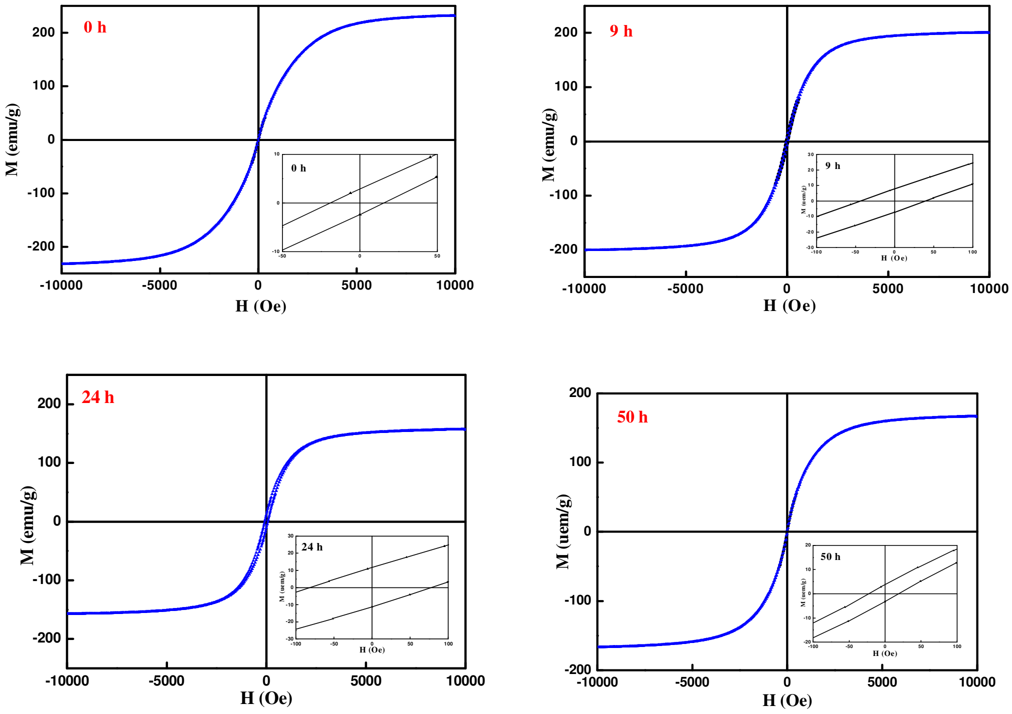

Fig. 4. Hysteresis loops dependence on milling time of the Ni-Cr powders. The insert is an enlargement of the low field region.

Fig. 5 displays the coercivity changes of the Ni-Cr powder during the milling process. Hc increases to 60 Oe after 3 h of milling (i), decreases between 3 and 12 h of milling (ii) and increases to about 80 Oe after 24 h (iii). The increase of H_c during the early stage of milling can be related to the plastic deformation effect introducing internal strains and different types of defects such as dislocations, inclusions, particles interaction and surface irregularities which serve as pinning sites for the magnetic domain wall movement. The decrease of H_c during the second stage of milling might be attributed to the crystallite size refinement and to the bcc-Ni volume fraction reduction. The increase of $_C$ between 12 and 24 h of milling can be ascribed to the formation of the hard Ni(Cr). Another probable reason for the H_c behavior is the fragmentation of the magnetic particles during the milling process leading to a heterogeneous ferromagnetic structure where the Ni-rich ferromagnetic grains are separated by non-magnetic Cr and/or Cr-rich phases. Consequently, the coupling between the ferromagnetic grains becomes less effective, giving rise to the recorded hardening.

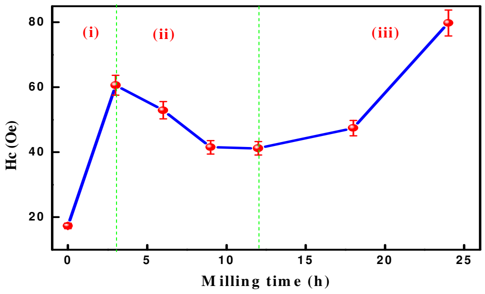

Fig. 5. Dependence of the coercivity, Hc, with milling time.

The saturation magnetisation (M_s) change during the milling process is shown in Fig.6. The decrease of M_s suggests significant magnetic moment change during the alloying process due to the modification of the nearest-neighbour configuration of the Ni. Indeed, the existence of non-magnetic Cr atoms in the vicinity of Ni ones leads to the reduction of the magnetic moment per atom and therefore, to the magnetization reduction. The obtained values of the saturation magnetization and the coercivity of about 157.3 emu/g and 80 Oe, respectively after 24 h of milling are higher than those reported for the ferromagnetic amorphous Ni-Cr alloy prepared by rapid cooling from the liquid state where Ms = 6.8 emu/g and H_c = 3 Oe. The comparison with our results suggests that the elaboration conditions influence strongly the structure and microstructure of the end product and therefore, the magnetic properties.

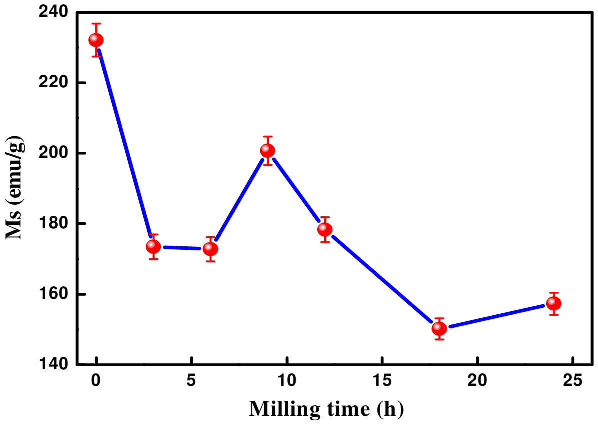

Fig. 6. Saturation magnetization variation versus milling time.

The remanence-to-saturation ratio, M_r/M_s which is about 0.04 after 24 h of milling, indicates that small magnetic particles are typically single domains. This result is in a good agreement with that observed in the $Ni_{50}Co_{50}$ [10] binary alloy produced by high energy ball milling process.

3.3. Microhardness

The powder compressibility is generally affected by particle shape, particle size and distribution, surface oxide layer, impurities, amount of solid lubricant added, chemical composition and work hardening.The powder aptitude to formability is favoured by (i) the presence of a great number of free surfaces with high interfacial energy providing short diffusion path which contribute to cold welding under the applied pressure; (ii) frictional force between powder particles and the wall of the die dissipating a power responsible for tool temperature increase up to 90°C which leads to the increase of the contact number between particles; (iii) the insertion of small and spherical particles in the stacking of the large ones minimize the unoccupied space.

The Vickers micro-hardness and the porosity evolutions versus milling time of the compacted Ni-Cr powders are shown in Fig. 7 The micro-hardness of the powder particles increases linearly with increasing milling time. At the first stage of milling, the sliding of atomic plans imposed by plastic deformation occurs by dislocations movement having a low density. As the milling process progresses, the grain size is reduced and the deformation occurs in the shearing bands located in the powder particles. The reduction of grain size leads to the increase of the particles resistance and therefore to the yield stress and the micro-hardness increases. In addition to the work hardening, the increase of micro-hardness is indicative of the substitution of Cr by Ni and the formation of the Ni(Cr) solid solution. The H_V value obtained after 24 h (176 H_V) is lower than that recorded in the ball-milled Fe-30Co powders (450 H_V) [12]. In Fe-C-Cu-P, the micro-hardness varies with C content (0.2 - 1 %) and applied pressure (400-700 MPa) [12]. It has been shown that hardness is strongly influenced by the porosity percentage. Indeed, for the compacted Fe-0.35P-0.35Cr powder with porosity of about 3 %, the hardness is about 168 Hv while in the case of Fe-0.7P- 0.7Cr with a porosity of about 7 %, the hardness reaches a value of about 189 Hv [13]. The porosity is relatively low for the short milling periods because of the weak dislocations density and low hardness. Consequently, the powder particles aptitude to be plastically deformed is important since the plastic deformation increases the number of contact between grains which leads to the decrease of the interior grain porosity. The obtained pellet after 50 h of milling with a porosity percentage of about 42 % was partially exhausted. This behaviour can be attributed to the strong frictional force and to the grains inaptitude to create mechanical liaisons and to resist to residual strains during ejection from the die. In the case of the compacted Fe and Cu with porosity fraction of about 15 %, both transmission electron microscopy and XRD analyses revealed the absence of plastic deformation. For cupper, the plastic deformation takes place entirely by means of grain boundary sliding in porosity free which is associated with a reduction in the elastic modulus of disordered grain boundaries which are considered elastically softer than the grain interiors [14].

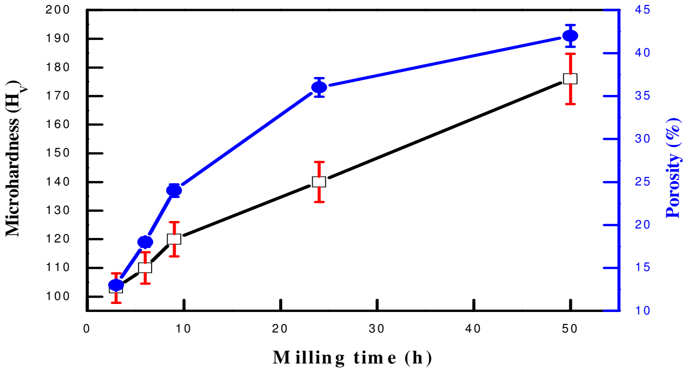

Fig. 7. Evolution of Vickers micro-hardness and porosity percentage versus milling time.

Conclusion

Nanostructured Ni60Cr40 powder mixture was prepared by mechanical alloying. The reaction between Ni and Cr leads to the formation of disordered Ni(Cr) and Cr(Ni) solid solutions in addition to Ni after 6 h of milling. Morphological observations show a broad shape distribution of the powder particles. The elemental mixing powders kinetics can be described by an Avrami parameter n = 1.1 and a constant rate k = 0.12. Both porosity percentage and Vickers microhardness of the compacted powders increases with structural refinement.

Acknowledgement - The authors are very grateful to A.M. Mercier from the Laboratoire des Fluorures, Université du Maine, Le Mans, France for the XRD measurement.

References

1. Neishi K., Uchida T., Yamauchi A., Nakamura K., Horita Z., *Mater. Sci. Eng. A* 307 (2001) 23.
2. Valiev R.K., Islamgaliev I.V, *Prog. Mater. Sci.* 45 (2000) 103.
3. Dekhil L., Alleg S., Suñol J.J., Greneche J.M., *J. Adv. Powder. Technol.* 20 (2009) 593.
4. Alleg S., Kartout S., Ibrir M., Azzaza S., Fenineche N.E., Suñol J.J., *J. Phys. hem Sol.* 74 (2013) 550 .
5. Bensebaa N., Loudjani N., Alleg S., Dekhil L., Suñol J.J., Al Sae M., Bououdina M., *J. Magn. Magn. Mater.* 349 (2014) 51.
6. Kurata Y., Tsuji H., Shindo M., Nakajima H.. *J Nucl. Mater.* 246 (1997) 196.
7. Bezzon Osvaldo L., Pedrazzi H., Zaniquelli O., da Silva T., Bose C.. *J. Prosthet. Dent.* 92 (2004) 274.
8. Baran G.R. *J. Prosthet. Dent.* 50 (1983) 639.
9. Taggart W.H. *Cosmos.* 49 (1907) 1117.
10. Loudjani N., Bensebaa N., Dekhil L., Alleg S., Suñol J.J., *J. Magn. Magn. Mater.* 323 (2011) 3063.
11. Laala-Bouali H., Bentayeb F. Z., Louidi S., Guo X., Tria S., Suñol J.J., Escoda L., *J. Adv. Powder. Technol.* 24 (2013) 168.
12. Lindskog P., *J. Powder. Metal.* 16 (1973) 374.
13. Jiten D., Chandrav, Misra P.S., Sarma B., *J. Magn. Magn. Mater.* 320 (2008) 906.
14. Sandim M.J.R., Stamopoulos D., Sandim H.R.Z., Ghivelder L., Thilly L., Vidal V.. *Conduc. Sci. Technol,*19 (2006) 1233.

(2015) ; http://www.jmaterenvironsci.com